Metamaterial Shaped LANR-Cathodes Produce Deuteron Flux

Mitchell Swartz*

Abstract — **Metamaterials and "lattice assisted nuclear reactions" (LANR) defy previous expectations. Yet each produces solid, experimental results. The motivation for this effort was to discover why one physical structure of LANR devices in high electrical impedance solution was one of the best arrangements for efficiency. The analysis shows that from the stereoconstellation of the electrode system, a unique E-field distribution is generated, linked to intrapalladial deuteron flux.**

I. METAMATERIALS AND LANR DEFY EXPECTATIONS

Metamaterials[1-24] and "lattice assisted nuclear reactions" (LANR)[25-42,90] have surprising, important physical characteristics that defy previous expectations and conventional thinking. Yet each produce solid, indelible experimental results. Metamaterials, with precise engineering structures, have characteristic behavior far beyond their normal expected responses, making previously "impossible" effects such as negative refractive index[1,2] and electromagnetic cloaking[3] occur. Similarly, reports of excess energy and nuclear reactions from solid state LANR[25-42] were initially felt to be impossible, but growing experimental evidence suggests otherwise. Active LANR devices produce helium-4,[25,26,35,46] tritium,[27,28,31,33] small amounts of radiation,[29,30] and fractions of a megajoule of "excess heat" per day.[37,39,41]

The motivation for this effort was to find out why these cathodes (with their helical structure and high electrical impedance solutions) are one of the best arrangements for efficient LANR devices.

Recognition that metamaterial behavior might be involved in the most efficient of LANR devices has led to the present investigation and paper. Metamaterials will be introduced here because their mere existence proves there may be more to think about than present well-known material properties. The range of materials will be discussed for the optical materials just to show the range of diversity. Nature is complicated. In the case of LANR investigations, certain shapes, sizes, configurations, and background solution resistances led to superlative LANR behavior as judged by heat produced. This is metamaterial performance above material science alone.

The present analysis has revealed that loading and intrapalladial deuteron flux are linked to successful LANR results and they result secondary to the stereoconstellation of the electrode system and the E-field that is generated. The findings are of importance to the design of new electronic devices using LANR cathode metamaterials, providing new ways to direct intrapalladial deuteron transport, similar to semiconductor electrons and holes. What makes this interesting for both LANR and other experimental fields is that in this century, attention must be paid to shape, configuration, stereoconstellation, and not simply bulk and surface material properties.

A. Metamaterials

Metamaterials can create negative refractive index materials,[1,2] electromagnetic cloaking (and not just screening),[3] a simultaneous negative phase and group velocity of light,[4] anomalous reflections and excitations of surface waves,[5] isotropic lenses,[6] and soliton decoherence.[7] Electrical permittivity, e, and magnetic permeability, μ, are both positive in nature.[8] In such normal materials, classic principles use the right-handed rule for electromagnetic (light) propagation, with the energy (Poynting vector[9]) traveling in the same direction. However, a "left-handed material" (LHM) has a negative (refractive) index material (NIM), and other unusual things occur. In LHMs, both e and μ are negative, and the phase and group velocities of light propagate opposite[10,11] the Poynting vector (energy flows), with reversal of the expected Doppler shift. Cherenkov radiation, normally emitted forward, is emitted backwards.[12]

Metamaterials come in both arrays,[13-16] sol-gel composites.[17] They are useful in electrical engineering, making novel antennas, filters, waveguides, and artificial magnetic media, composed of a split-ring resonator (SRR) lattice with negative permeability over a certain frequency range.[14] For X-band, the SRRs and wires are arranged into a two-dimensional structure with a 5 mm lattice parameter. Terahertz metamaterials are composed of conducting SRRs and wires on thin fiberglass circuit board material, arranged in a regular array of cells. Metamaterials have been engineered in the optical to mid-IR range with fabrication by nanoimprint lithography,[18,19] using perforated SiC membranes,[20] into broadband devices of right/left-handed metamaterials.[21] Devices have even been designed using planned zero refraction metamaterials,[22] and second-harmonic generation from magnetic metamaterials.[23,24] The important point is that metamaterials, through their unique, novel structures, can

make previously "impossible" effects occur. Conventional metallurgy and material science accrue from the "internal structure of cathode material," whereas metamaterials result from the precisely crafted and planned external structure.

B. Lattice Assisted Nuclear Reactions (LANR)

For two decades, worldwide experimental LANR results[25-42] have provided compelling evidence that nuclear reactions are assisted by a lattice.

LANR are nuclear reactions assisted by a metallic lattice, if it is loaded with the substrate of the reaction as an isotopic fuel, in the form of an alloy, such as PdD_x and triggered with other factors, not all of which have been elucidated at this time. These include an adequate deuterium flux, a high enough deuteron loading ratio D/Pd,[43-45] and a sufficient applied electric field intensity. Although the underlying physics and pathways are not fully understood, nuclear reactions and excess heat occur for input energy levels of less than 10 to several hundred eV into an active LANR system or device.

Active LANR devices produce nuclear products, such as heat-commensurate helium-4,[25,26,35,46] tritium[27,28,31,33] with production rates circa 3,000-7,000 atoms/sec, new elements of Al, Mg, Ca, Si, Zn, and Fe,[47] other isotopes and very small amounts of radiation of alpha and proton emissions, and rare neutrons of energies exceeding 12 MeV.[29,30] Accompanying penetrating radiation emissions, when found, have broad Bremsstrahlung energy distributions, with an occasional Pd K-shell peak at 20 keV. The excess heat, radiation emissions, and tritium production can be sporadic or occur in bursts. When active LANR devices demonstrate excess energy as the production of more output heat than an ohmic control ("excess heat"). This can be hundreds of thousands of joules of 'excess heat' per day. The produced energy is of a magnitude beyond that which was applied. IR imaging and thermometry (SPAWAR and JET Energy) indicates that the heat source is the cathode in discrete localized hot spots on the electrode's surface (Szpak in the medical thermal IR[28,48]), associated with mini-explosions (detected by SPAWAR using piezoelectric crystals attached beneath the cathodes). Near-infrared imaging has revealed possible non-thermal near-IR emissions correlated with excess heat.

We have used proprietary driving systems to successfully run hydrogen- and deuteron-loaded electrodes (nickel and palladium high electrical impedance [$Pd/D_2O/Pt$, $Pd/D_2O/Au$, $Ni/H_2O_{1-y},D_2O_x/Pt$, $Ni/H_2O_{1-y},D_2O_x/Au$]) and codepositional [$Pd/Pd(OH)_2/Pt$] LANR devices. Figure 3 shows a close up of an active cathode. The cylindrical anode, parallel oriented spiral helix cathode, and several metallic, electrically insulated, rods collecting data appear normal. In a unique manner, the high impedance solution located between the two electrodes also bathes the Phusor™ spiral cathode in the inside region, outside the cylindrical spiral palladium lattice, but within the circumference spanned by the helix. Some metamaterial spiral Pd LANR devices in heavy water, after pretreatment, have exhibited impressive energy gain and fairly good reproducibility[37,39,41] at the multi-watt input power level with power gains to ~>230% and higher. Driven at their optimal operating point (OOP), they show excess energy gains of 1.2 to more than ~3, with excess power to several watts.[37]

The excess heat can only have a nuclear origin because its magnitude is beyond the chemical energies available even by including all reactants and their containers, and is beyond that exhibited by an ohmic control resistor in the same electrical circuit.

Excess heat (Swartz, Fleischmann, Miles, Bockris) and helium-4 are the usual products (Miles, Arata, Case), but very low levels of charged particles, tritium (Srinivasan, Bockris, Szpak, Storms), low energy (<20 keV) ionizing radiation (Miles, Srinivasan), and even rare neutrons have been detected (Srinivasan, Boss, Forsley).

As a result of these findings, the reaction—ignoring the phonons, vacancies, lattice, coherence—is something like:

$$D + D \rightarrow He_4 + \sim 22 \text{ MeV (lattice)}$$

The excess power per unit area is greater than 2.9 to 12 watts/cm^2. The excess power density is in the range of 100-1,000 watts/cm^3, 15 to 150 times greater than was initially announced in 1989.

Historically, LANR—a potentially very important form of hydrogen energy production—became investigated after March 1989, when most attention was misdirected to its messengers,[36] in part because nuclear fusion had never been achieved in a metal lattice, not to mention near room temperature. Most high energy theoretical physics did not involve a lattice in any calculation. As a result, the initial positive reports were erroneously thought to be in disagreement with the accepted theory of nuclear reactions, even though efforts were made to demonstrate that gamma emission was in fact spin-forbidden,[49] that Mossbauer effect had heralded the nucleus-lattice coupling,[50] and that the lack of penetrating ionizing radiation was consistent with conventional physics.[50-52] Most early LANR efforts failed and success of LANR has been difficult to achieve for a number of reasons, including lack of good paradigms,[53] improper cell configurations, lack of pure metals of sufficient integrity able to load and maintain sufficient hydrogen without leaking (able to reach D/Pd ratios > 0.85), improper pretreatment, the presence of protium and other contamination by materials which quench performance, inadequate loadings, inadequate incubation and confinement times (sometimes weeks),[45] inadequate deuteron flux,[54,55] supplying the requisite activation energy while maintaining structural lattice integrity, inadequate phonon support,[50] and a variety of patterns of failure.[45]

Perhaps most important has been the need to electrically drive the devices at, or near, their OOP (that point along the input power axis where driving the LANR device yields maximum output of product[56-58]) for peak excess heat production. The OOP manifolds, seen by analyzing the results of a LANR experiment by input electrical power, have wide generality for LANR reactions. Their use organizes an otherwise disparate field where results make them more reproducible. If an LANR system is operated far outside of its OOP, it will not be active.[45] The desired reactions have slowly become more reproducible, controllable, and of higher power density. We have found that possible excess heat measurements in metal deuterides is easier and more reproducible when false positives are ruled out by adequate Nyquist sampling, noise measurement, thermal waveform reconstruction, time-integration, thermal ohmic and dual ohmic controls, and the

other techniques to obtain thermal power spectrograms. The research uses redundant calorimetry with up to six independent methods to evaluate, and certify possible anomalous heat,[37-39,41] four-terminal conductivity measurements of the loaded cathode, and traceable heat flow measurements.

C. Does Phusor Structure Create Material Properties?

We have tried many designs and variations of electrodes, arrangements and materials, but the uniquely-shaped spiral Phusor™ cathodic structure has stood out for reproducibility, activity, and power gain, for several Group VIII materials. Its arrangement and stereo-constellation of electrodes appears to be one of the best arrangements for a LANR system, measured by activity and power gain.[37-39,41] We previously reported that unique well-localized, small-area bubble coverage has been correlated with successful LANR-active $Pd/D_2O/Pt$, $Pd/D_2O/Au$, and $Ni/D_2O,H_2O/Pt$ device operation. This has been confirmed by heat flow measurement, calorimetry, electrical and mechanical energy conversion devices, and dual serial calorimetry.

This type of LANR device, with its helical, cathodic design and low electrical conductivity solution, is the most successful half-electrochemical system we have found judged by robust excess heat production and reproducibility. Why? Our hypotheses for its superior function included the cold working, preparation, Frenkel defects, and the possibility of specific alterations in the electric field intensity distribution. Also, metamaterials may have begun in the optical and microwave areas but we elected to take a closer theoretical, calculated look at their use for energy production and conversion. We began a theoretical investigation which indicates that our best LANR devices may be a metamaterial.

II. EXPERIMENTAL SIMULATION

A. Experimental — First Order E-field Analysis

Given the relative impedances involved, it is likely that the results of the simulation described are initially close to what occurs in the experimental setups. Metamaterials have been studied using *ab initio* numerical simulation.[59] In other non-metamaterial systems, electric field intensity computations using Laplace's equation for a variety of geometries[9,60,61] are well known. Important considerations include that of a "Conducting Circular Rod in Uniform Transverse Field" and "Approximate Current Distribution around Relatively Insulating and Conducting Rods."[60] More complicated systems have been analyzed in several ways. Such electric field computations have been undertaken by numerical analysis of the polarizability characteristics for dielectric circular cylinders through an integral equation for the scalar potential.[62] This is done by calculating the polarization charge surface density in a Fourier series, with the related coefficients (the so-called multipoles) obtained from a linear set of equations,[63] by analytic calculation for two parallel dissimilar cylinders using a linearized Poisson-Boltzmann equation,[64] by adding to the Poisson-Boltzmann equation further consideration of the electrostatic potential and the energy of such a charge distribution,[65] by a two-term Galerkin solution for a hollow, conducting tube of finite length held at a fixed potential,[66] by a conformal mapping that converts the actual boundary-free field zone into a rectangular domain,[67] by imaging,[68] and by dyes sensitive to electric potential.[69]

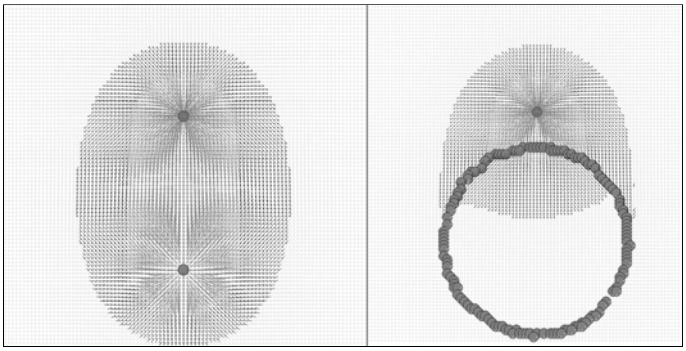

Figure 1. Two-dimensional E-field distributions.

For the present investigation, a set of experiments were set up to theoretically determine why the metamaterial setup gave superior results. Examined was the effect of geometric parameters, of both the wire-wire and wire-Phusor™ system (Figure 1), upon the electrical field distribution. Our gendanken computed simulation used Laplace electrostatic calculations away from the electrodes, away from the interface, and outside the double layers. There are limitations in this analysis. First, only *ab initio*, first order electric field distributions were qualitatively examined for obvious differences that might be present secondary to structure. The goal was not to perform a quantitative Gouy determination, nor to examine near surfaces, nor in double layers. Second, no closed-form solution probably exists because this is a dynamic system with secondary dielectric effects because conduction and polarization are linked (through Hilbert space[8]), and because of convection, and time variant thermal and Bernard instability issues. These were a first order extension of the previously described and successful Q1D model of isotope loading,[54,55] to now include intrapalladial deuteron flow, similar to holes and electrons in semiconductors, within the loaded electrode.

Although classical electrostatics indicates that a perfect conductor does not have an electric field within it, the real palladium cathode is not a perfect conductor. We measure the palladium electrical conductivity by four terminal measurement which, for these Phusor™ cathodes, ranges from 40 to ~120 milliohms. This theoretical examination considered the Phusor™ type LANR Pd spiral, immersed and bathed, like the platinum anode, in the high electrical resistivity solution, relatively electrically insulating, for the most general case of two infinitely long electrodes, placed in a vertical, parallel position. We modeled the device as an electrically conductive ring of cylindrical symmetry (open at some angle for each 2D cut) of infinite length. Using boundary conditions and superposition, the electric field distribution was calculated to first order, qualitatively, in 2D.

III. RESULTS — E-FIELDS SUGGEST METAMATERIAL

The spiral LANR device is a metamaterial, and its physical structure enhances the metallurgic properties of loaded palladium. This alters the electric field distribution, producing continuous deuteron flux within the loaded palladium. This is unique to the Phusor™ LANR device, creating a distinguishing electric field distribution different from customary wire-wire and other systems. The electric field distributions derived are shown in Figure 1, which shows in cross-section the derived first order two-dimensional vector electric field distributions for the two cases.

The first case is that of two parallel, infinitely long wire

electrodes (anode at the top, and cathode below). The second case is a wire-Phusor™ system. In cross-section, the Phusor™ complex structure is approximated. The anode is at the top, and the cathode in each pair is located below it. In these simulations, each cathode is electrically polarized against, and physically located opposite, an anodic wire of platinum. Color variations (not shown here) show several arbitrary thresholds in electric field intensity.

The results of this analysis show the 2D E-field distribution and deuteron flux sequelae vary greatly between the wire-wire system and the wire-Phusor™ system. The 2-D E-field distributions reveal there are important differences between the electrostatic distributions produced by the two arrangements. In a 2D view around the cathode wire, there is a near isotropic distribution of the E-field. With the Phusor™, there is not. The configuration examined in this present investigation has revealed that in the helical system there is a direct loading, electric field intensity which results in those portions of the cylinder which are closest to the wire extending over a solid angle over a two dimensional angle of approximately ~45° - 130°, depending on many factors of the Phusor™ geometry and precise inter-electrode distance. The result is a clear deuteron flux through that portion of the cathode, which does not characterize the two wire situation over as large a volume. With the metamaterial configuration, there is a flux of deuterons resulting in a quite different performance than conventionally described, or expected, in electrochemistry using simpler structures such as wires. Referring to Figure 2, consistent with electrostatics, the fluxes of deuterons in the solution (J_D) and in the metal, both for loading (J_E), gas evolution (J_G), and fusion (J_F) are now augmented by an equilibrium intrapalladial deuteron flux (J_{IP} in Figure 2); therein a possible rub for hydrogen isotope energy production reactions.

IV. INTERPRETATION OF SIMULATION

A. E-Field Distribution Change

Our previous experimental results determined that the spiral helical structure and geometric arrangement of the palladium Phusor™, located opposite a platinum anode, can yield unusually high excess heat. That led to the present theoretical analysis which has determined that the uniqueness of the Phusor™ cathode—with its open helical geometry and orientation in a high electrical resistivity solution—alters the 2-D electric-field intensity (E-field) spatial distribution uniquely and perhaps enables the desired reactions to occur. The pericathodic E-field distribution becomes less isotropic in two dimensions. The portion of the cathode vicinal to the anode, off axis, may sustain a higher than normal internal electric field intensity within its bulk lattice volume.

B. Deuteron Flow Distribution Change

The metamaterial aspect of these LANR devices appears to enable them to be more fully loaded, and the structural geometry interacting with the applied electric field intensity produces a net continuous flux of deuterons moving through the palladium. With the metamaterial Phusor™ LANR cathode there is an equilibrium intrapalladial deuteron flow, in addition to, and after, deuteron loading through portions of the cathode. Two deuteron flows are created by the Phusor™. First is the standard deuteron inter-electrode (between electrodes) loading flux, beginning in the solution and ending in the metal lattice. This is driven by the applied electric field intensity. Second, there is an additional intraelectrode deuteron flux, through the metal itself. This intrapalladial deuteron flow continues at equilibrium, similar to the microscopic equilibrium semiconductor flux of holes and electrons at a p-n junction. We now suspect that this additional type of deuteron flow is critical and enabling to LANR results. The results here support this. So do the results of Violante[46] and Iwamura.[34]

C. Deuteron Flux

This is where the simulation must cross the boundary conditions with what is observed. The next three sections explain a successful model (the Q1D, or quasi-1-dimensional model of isotope loading) which has explained some of LANR's complexities. The three sections after that build upon one of the models' teachings to explain how the metamaterial findings support the observed superior performance for such shaped electrodes.

Deuteron flux has been examined in metal scandium films, where buildup of deuterium in the near-surface area is controlled by migration to deeper depths,[70] in niobium membranes,[71] and in molybdenum, below 500 K, deuterium retention is enhanced by trapping at defects produced by the deuterium bombardment; above 500 K, the implanted deuterium is immediately released.[72] There has been a need to study these deuterium fluxes in palladium systems. Nernst calculations of the activities of electrolyte[73,74] adjacent to a metal electrode have been applied to LANR[36] to derive distributions of deuterium in the palladium[30] and solution.[54,76] However, the LANR systems are not at equilibrium, and Nernst calculation may not be applicable.[54,55] Also, a vicinal reference electrode may herald the Nernst potential, but probably not the loading flux rate (which will be shown below to be key to these reactions). Therefore, a Q1D model for hydrogen loading of an electrode was formulated[54] which does not require equilibrium for accuracy. The Q1D model describes the loading flux of hydrogen by the ratio of two energies (electric order to thermal disorder ratio).

Figure 2 is a schematic, simplified representation of the anode, solution, and a portion of the cathode along with five types of deuteron fluxes involved in loading, D_2 evolution, and putative fusion—in solution and the palladium. The figure shows the deuteron cationic flow (J_D), and the four types of deuteron flux in the loaded palladium cathodic lattice (J_E, J_G, J_F, and J_{IP}). Deuteron flux (J_D) begins far from the cathode surface, in the deuterium oxide (heavy water) located between the electrodes, where the deuterons are tightly bound to oxygen atoms as D_2O. There is no addi-

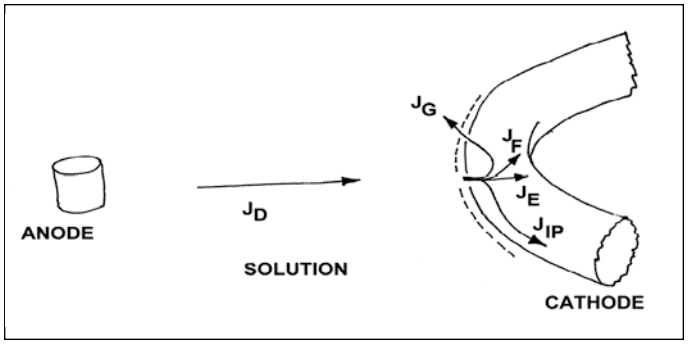

Figure 2. Schematic model of deuteron flux.

tional solute. In the absence of significant solution convection, the flux of deuterons (J_D) results from diffusion down concentration gradients and electrophoretic drift by the applied electric field.[54,77] Cationic deuteron flux (J_D) brings deuterons to the cathode surface, from the heavy water as D-defects[78,79] are driven by the applied electric field intensity to create a cathodic fall and double layer before the electrode surface. From the metallurgical point of view, from the metal surface, atomic deuterons either enter the metal (are "loaded"), remain on the surface, or form diatomic deuterium gas bubbles (D_2). The gas bubbles (D_2) are undesirable producing low dielectric constant layers in front of the electrode, obstructing the electrical circuit. And so, at the metal surface, four components of deuteron flux must be considered,[54,55] fundamental to the entire understanding of these phenomena. These deuteron fluxes include entry into the metal (J_E), movement to gas evolution (J_G), and an extremely tiny loss by potential fusion reactions (J_F). There is conservation of deuterons with the exception of a loss (J_F) to all putative fusion reactions, which are extremely small, if present. With this paper, we now add the concept of a continuous, equilibrium, flux of deuterons within the cathode (J_{IP}), which may be consistent with excess heat and an observed unusual bubbling pattern (see below). The important point is that different deuteron fluxes must be distinguished[54] at the surface of the low hydrogen-overvoltage palladium, with its surface populated with atomic, diatomic (D_2), and bulkentering deuterons.[80,81] This paper expands the Q1D model of loading to include the possibility of intrapalladial deuteron flow at equilibrium.

D. LANR is NOT Electrolysis

From the mathematical point of view, the three components of flux are the entry of deuterons to the lattice (J_E), gas evolution (J_G), and the desired fusion reactions (J_F). Dividing each flux by the local deuteron concentration yields the first order deuteronflux constants, k_E, k_G, and k_F [cm/sec], respectively, which are the basis of the rest of the discussion, and Equation 2:

$$J_D = -B_D * \frac{d[D(z,t)]}{dz} - \mu_D * [D(z,t)] * \frac{d\Phi}{dz} \qquad (1)$$

The deuteron flux, J_D, depends on deuteron diffusivity (B_D) and electrophoretic mobility (m_D), and the applied electric field intensity. At any molecular site across the heavy water solution, the applied electrical energy is a tiny fraction compared to k_B*T, so the deuterons migrate by drift ellipsoids of L- and D-deuteron defects in the applied electric field creating a ferroelectric inscription.[78,79] This D-defect conduction/polarization process augments other charge carriers, ionic drift, space charge polarization, and clathrates. The resultant D-defect migration produces a "cathodic fall" of deuterons and an E-field contraction so that most of the voltage drop is at the interface in front of the electrode surface. This concentration polarization may produce very large local electric field intensities, possibly ranging from 10^4 to 10^7 volt/cm.[54] From the concentration polarization of deuterons before the cathode, the Pd loads, controlled by the double layer, limit the entry of deuterons to the metal surface. At the inner boundary of the double layer, intermolecular deuteron transfer from the heavy water solution to the metal surface, coupled by electron-limited transfer, leaves an atomic deuteron on the metal surface. This leaves an atomic deuteron attached to the metal surface, and the electrode metallurgy controlled by the tiny interfacial region, which might be less than 10 Angstroms thick, by the applied electric field intensity, and by the local concentration of deuterons. The entry to the palladium surface is driven by infrared vibrations and microwave rotations,[54] creating a solution photosensitivity which produces a photoactivated increase of excess energy and loss of power gain.[42] Palladium has its surface populated with atomic (D) and diatomic deuterium (D_2). A large number of those deuterons can also enter the metal, forming a binary alloy.[80,81] Deuterons which enter (load) into the palladium lattice are "dressed" by a partial electronic cloud, shielding their charge (Born-Oppenheimer approximation). The deuterons drift along dislocations and through the lattice and its vacancies, falling from shallow to deeper located binding sites. There is obstruction by ordinary hydrogen and other materials at interfaces and grain boundary dislocations.

$$K_e = (\mu_D * E) - (K_g + K_f) \qquad (2)$$

Equation 2 is the deuteron loading rate equation. It relates cathodic deuteron gain from the applied electric field to the loss of deuterons from gas evolution and fusion, and teaches many things. The deuteron loading rate equation shows that the deuteron gain of the lattice [through the first order loading flux rate (k_E)] is dependent upon the applied electric field *minus* the flux rate losses of deuterons from gas evolution (k_G) and fusion (k_F). The deuteron loading rate equation, Equation 2, reveals that desired LANR reactions are quenched by electrolysis, which is opposite conventional "wisdom" that LANR is "fusion by electrolysis." It also heralds that LANR can be missed by insufficient loading, contamination (effecting k_E, *e.g.* by protium), and by the evolution of D_2 gas, which inhibit the desired reactions.[54]

$$K_e = \frac{B_D * qV}{L * [k_B * T]} - (K_g + K_f) \qquad (3)$$

The modified deuteron flux Equation 3 is changed by substituting the Einstein relation, which makes for an equation reminiscent of semiconductor physics at p-n junctions. The first term now has geometric, material factors, and the ratio of two energies (the applied electric energy organizing the deuterons divided by k_B*T, thermal disorder). The modified deuteron flux equation reveals how competitive gas evolving reactions and the applied electric field energy to thermal energy [k_B*T] are both decisive in controlling the deuteron loading flux in palladium. Successful LANR experiments are dominated by this ratio reflecting the "war" between applied electrical energy which is organizing the deuterons versus their randomization by thermal disorganization. The two terms are the first order deuteron loss rates by gas evolution and the desired fusion process(es). Thus, this may be similar to holes and electrons in semiconductors, and their equations involving the Einstein relation (*cf.* Equation 3) are also similar. The Phusor™-cathode is a unique LANR metamaterial, whose stereoconstellation connects deuteron loading to other fluxes of deuterons continuing to move inside of the palladium, just as holes and electrons move in a semiconductor. Second, Equation 3 is similar to some flux equations from semiconductor physics, so there is the question of sim-

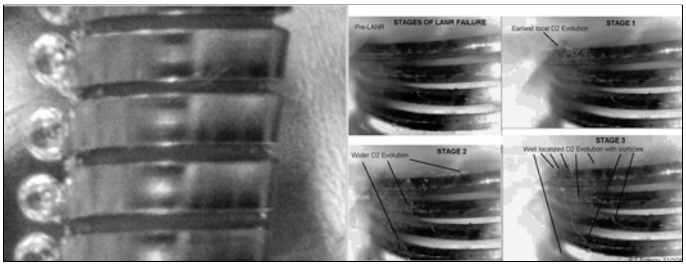

Figure 3. Active and inactive Phusor™ cathodes.

ilarity of deuterons in Pd to holes and electrons in semiconductors. Third, this metamaterial view of cathodes may explain their relatively-reproducible excess energy production compared to other LANR systems, thereby opening up new routes to improved hydrogen energy production by LANR. Finally, although not all of the controlling factors of LANR success have been elucidated, this paper adds a new control point—deuteron flux within the lattice from an applied electric field intensity within an electrochemical LANR cell.

E. Experimental — Role of Bubble Coverage

Bubble formation has a large controlling role in electrochemistry[82] because the adhering bubbles isolate the electrode.[83] At high current densities, bubble evolution is a rate limiting step, dependant upon whether the bubbles coalesce or not.[84] Under microgravity conditions or if acidic solutions are used, large bubbles are formed, coalesce and remain on the cathode surface.[85,86] Alkaline solutions make a bubble froth.[86] This is also true with LANR. The bubbles interfere with competitive reactions, including loading and reduction (*e.g.*, ferricyanide on Pt).[87,88] The activation energy is in the range of 56 kJ mol-1 (electrodeposited Ni on Pt) to 204 kJ mol-1 (electrodeposited Hg on Pt).[89]

F. Bubble Coverage

Figure 3 shows a close-up of an active Phusor™ spiral-wound excess-heat-producing palladium cathode. The Pt anode is to the left of the cathode, and is not shown in the photograph, as discussed in detail.[37] A high electrical resistivity solution, located between the two electrodes, bathes the Phusor™ spiral cathode, including within the spiral. There is seen very limited, well localized, small area large-bubble (asymmetric) coverage bubbling vs. normal bubbling.[37] There are bubbles only on one side of the cathode, what we call "asymmetric bubbling," which differs from normal bubbling. With LANR success, at current densities of 1.5 x 10^{-4} to ~0.13 amperes/cm^2, we have observed behavior similar to what is seen in microgravity or acidic solutions. This is seen at relatively high voltages. Plasmas have not been observed, unless the Phusor-cathode, or anode, are removed from the solution during the run. We postulated in 2003 that this unique type of cathodic bubble behavior—"asymmetric electrolysis"—heralds, and drives, intrapalladial deuteron flux through that portion of the loaded metal cathode. Thus, it could be seen as a sign of LANR success for some excess heat—producing cathodes as experimentally observed and reported, and openly demonstrated at ICCF10.[37,41] The present paper goes further and provides confirmatory theoretical and experimental support (Figures 1,3). First, this paper reports that Phusor™-generated metamaterial-derived intrapalladial flux in the cathode does appear to be heralded by a small bubble evolving area on the surface of palladium and linked to activity of LANR cathodes (Figure 3). This putative hypothesized intrapalladial deuteron flux is corroborated with this paper whose results show the asymmetric electric field distribution at the front of the Phusor™ (facing the anode). Intrapalladial deuteron flux may have implications for palladium loading,[37,54,55] for monitoring that loading, and regarding the likelihood of success. By contrast, many electrochemists have generally been more concerned with "throwing power" of their systems and solutions, rather than focusing on improving active LANR behavior. Generally, in solutions of more electrical conductivity, with materials other than palladium, and with no possibility to load (or create other desired reactions), one sees—at hundreds of volts applied yielding a current density of ~10^{-5} amperes/cm^2—tiny bubbles over the cathode, beginning at select, preferred sites.

G. Diffuse Wide-Area Bubble Coverage

We have extended this effort to see where there is breakdown of this unusual behavior. How does it breakdown, by behavior, distribution, and quantity? The lower photomicrographs show the signs of Phusor™ LANR failure. This is also observed in solutions with high electrical conductivity, as small bubbles appear all over the entire cathode for current densities >10^{-5} amperes/cm^2. These images show a previously active codeposition DAP Phusor™-type device [Pd*/D_2O-Pd(OH)$_2$/Au, 7.7 millimolar Pd(OH)$_2$], now driven to the far right of its optimal operating point (38.1 milliamperes, 131.8 volts). At this OOP location, unwanted new, competing reactions appear. These reactions remove energy from, and compete with, the desired reactions, as hydrogen evolution takes the place of deuteron flux through the metal and loading. In stage one, a small group of sites on the Phusor™ cathode, located closest to the anode, begin evolving small bubbles of diatomic heavy hydrogen. In stage two, occurring at higher voltages, a wide number of sites begin contributing to the evolution of hydrogen gas (bringing the optimal operating point manifold back to unity performance, or worse). In stage three, at even higher voltages, this recruitment of additional gas-evolving sites continues, with sausage instabilities, vortices, and gouts of larger bubbles then appearing. These are the signs of failure, and the absence of flux through the metal.

Figure 3 shows close-up photographs of active and inactive Phusor™ cathodes. On the left is well localized, small bubble coverage. A sign of LANR success at the spiral-wound palladium excess heat-producing cathode is heralded by bubbles on only one side of the cathode. The Pt anode is to the left of the cathode, and is not shown. The right photographs show the signs of failure. These reactions remove energy from, and compete with, the desired reactions.

V. CONCLUSION

A. Experimental — E-Field and Deuteron Flow

The Phusor™ spiral cathode system-wire anode system, with its open helical cylindrical geometry, creates a unique and unusual electric field distribution. There is an anomalous effect in those portions of the cathode closest to the anode. In some configurations, this extends over an angle of circa 45°-130° degrees. This results in both interelectrode

deuteron flux from the solution to the electrode for loading, and intrapalladium deuteron flux (after full loading). There is the possibility that changes resulting from the geometry and stereoconstellation of the cathode material may be a factor, and may account for the relative success of the Phusor™ system. In addition, the understanding, and engineering, of these two types of deuteron flows is critical to new key components for successful LANR, and perhaps other hydrogen, energy production results.

B. Metamaterial Role in LANR

Geometry, stereoconstellation, and location of electrodes, metamaterial issues, are now shown to play additional possible roles in successful LANR experiments. The findings of this paper's theoretical research, supplementing much experimental work involving the Phusor™-heavy water system including with respect to spatial distribution of D_2 evolution and excess heat production, suggests that Phusors may be metamaterials. Here the electrode metamaterial function appears to help produce more successful and efficient LANR systems by generating additional types of equilibrium deuteron flux, a possible additional *sine qua non* for the desired reactions in successful LANR reactions. We believe that intra-electrode palladium flux is what is necessary to produce the desired reactions, and that such a flux is often missed in competing systems, based on our experimental results here, and a review of the poorer performance of some competing systems. Thus, there are several connections between metamaterials in general, these structures in particular, and then hydrogen energy devices in general, LANR devices in particular.

First, the results, theoretically and experimentally, suggest that in the pursuit of hydrogen energy, the metamaterial function may be important and augment the material properties by improving efficiency. The second important point is that in addition to past patterns of failure of LANR systems—from excessive electrical conductivity of the solution, to failure to drive the system near its OOP, to failure to adequately load—now metamaterial issues should also be considered. Third, consideration of metamaterial structure and stereoconstellation of the electrode system might engineer alteration of the two types of deuteron flows for the ultimate design of future, more successful, LANR materials and devices. In fact, researchers of LANR, hydrogen energy production systems, and the solid state have a new way to think about their systems, and a possible new spectrum of devices using intraelectrode deuteron flow. In the future, metamaterial intrapalladial flux may offer new types of devices (like p-n junctions). In LANR, theoretical contributions of metamaterial function should now be considered as a method to improve efficiency of actual experiments, and devices, and applications, in the future yielding an entire new spectrum of electronic devices using equilibrium intraelectrode deuteron flow and the products which result from that.

ACKNOWLEDGMENTS

The author thanks Gayle Verner for her meticulous help in manuscript and idea development, and Jeffrey Tolleson, Alex Frank, Alan Weinberg, Allen Swartz, Larry Forsley, Pamela Mosier-Boss, Brian Josephson, Brian Ahern, Jeff Driscoll, Isidor Straus, Michael Beigel, Steven Olasky, Scott Chubb, Peter Hagelstein and Richard Kramer for their helpful conversations, and JET Energy and New Energy Foundation for their additional support.

REFERENCES

1. Smith, D.R., Pendry, J.B., and Wiltshire, M.C.K. 2004. "Metamaterials and Negative Refractive Index," *Science*, August 6, 305, 788-792.

2. Grbic, A. and Eleftheriades, G.V. 2002. "Experimental Verification of Backward-Wave Radiation from a Negative Refractive Index Metamaterial," *Journal of Applied Physics*, 92, 10, 5930-5935.

3. Schurig, D. *et al*. 2006. "Metamaterial Electromagnetic Cloak at Microwave Frequencies," *Science*, November 10, 314, 5801, 977-980.

4. Dolling, G., Enkrich, C., Wegener, M., Soukoulis, C.M., and Linden, S. 2006. "Simultaneous Negative Phase and Group Velocity of Light in a Metamaterial," *Science*, May 12, 312, 5775, 892-894.

5. Brodin, G., Marklund, M., Stenflo, L., and Shukla, P.K. 2007. "Anomalous Reflection and Excitation of Surface Waves in Metamaterials," *Physics Letters A*, 367, 3, 233-236.

6. Verney, E., Sauviac, B., and Simovski, C.R. 2004. "Isotropic Metamaterial Electromagnetic Lens," *Physics Letters A*, 331, 3/4, 244-247.

7. Marklund, M., Shukla, P.K., Stenflo, L., and Brodin, G. 2005. "Solitons and Decoherence in Left-Handed Metamaterials," *Physics Letters A*, 341, 1-4, 231-234.

8. Von Hippel, A. 1954. *Dielectric Materials and Applications*, MIT Press.

9. Whinnery, J.R. and Ramo, S. 1953. *Fields and Waves in Modern Radio*, John Wiley & Sons.

10. www.fen.bilkent.edu.tr/~ozbay/Papers/60-02apl-LHMbayndir.pdf
www.fen.bilkent.edu.tr/~ozbay/Papers/70-03-ieee-ozbay_tap_2003.pdf
www.photonics.com/spectra/tech/XQ/ASP/techid.848/QX/read.htm
http://cetap5.mit.edu/metamaterials/papers/external/2004/Krowne_prl_2004.pdf
http://cetap5.mit.edu/metamaterials/papers/external/2000/smith.K_prl_2000.pdf
www.fen.bilkent.edu.tr/~ozbay/Papers/70-03-ieeeozbay_tap_2003.pdf

11. Chen, H. *et al*. 2003. "T-Junction Waveguide Experiment to Characterize Left-Handed Properties of Metamaterials," *Journal of Applied Physics*, 94, 6, 3712-3716.

12. Pendry, J. *et al*. Defense Advanced Research Projects Agency, http://physics.ucsd.edu/~drs, Air Force Office of Scientific Research.

13. Shelby, R.A., Smith, D.R., and Schultz, S. 2001. "Experimental Verification of a Negative Index of Refraction," Science, April 6, 292, 5514, 77-79.

14. Scott, C. and Cummer, S. "Towards Negative Index Material: Magnetic Response," www.ee.duke.edu/Academics/Undergraduate/IndStudy03/ScottC2003.html

15. Negative Index of Refraction In Left Hand Material Composite MetaMaterials Have Unnatural Electromagnetic Properties". what is Ref 15?

16. http://www-physics.ucsd.edu/lhmedia/how.html

17. Kielbasa, J.E., Liu, J., Ucer, K.B., Carroll, D.L., and Williams, R.T. 2007. "Sol-gel Nanocomposites as Metamaterials: Preparation and Optical Measurements," *Journal of Materials Science: Materials in Electronics*, 18, 435.

18. Wu, W. *et al*. 2007. "Optical Metamaterials at Near and Mid-IR Range Fabricated by Nanoimprint Lithography," *Applied Physics A: Materials Science & Processing*, 87, 143.

19. Wu, W. *et al*. 2007. "Mid-Infrared Metamaterials Fabricated by Nanoimprint Lithography," *Applied Physics Letters*, 90.

20. Korobkin, D. *et al*. 2007. "Mid-Infrared Metamaterial Based on Perforated SiC Membrane: Engineering Optical Response Using Surface Phonon Polaritons," *Applied Physics A: Materials Science & Processing*, 88, 4, 605.

21. Caloz, C. and Nguyen, H.V. 2007. "Novel Broadband Conventional- and Dual-Composite Right/Left-Handed (C/D-CRLH) Metamaterials," *Applied Physics A: Materials Science & Processing*, 87, 2.

22. Wu, Q. *et al*. 2007. "A Novel Flat Lens Horn Antenna Designed Based on Zero Refraction Principle of Metamaterials," *Applied Physics A: Materials Science & Processing*, 87, 2.

23. Klein, M.W. *et al*. 2006. "Second-Harmonic Generation from Magnetic Metamaterials," (4 versions) *Science*, July 28, 313, 502-504.

24. Linden, S. *et al*. 2004. "Magnetic Response of Metamaterials at 100 Terahertz," *Science*, November 19, 306, 1351-1353.

25. Miles, M.H. *et al*. 1993. "Correlation of Excess Power and Helium Production During D_2O and H_2O Electrolysis Using Palladium Cathodes," *J. Electroanal. Chem.*, 346, 99-117; Miles, M.H. and Bush, B.F.

1994. "Heat and Helium Measurements in Deuterated Palladium," *Transactions of Fusion Technology*, 26, December, 156-159.
26. Miles, M.H., Imam, M.A., and Fleischmann, M. 2001. "Calorimetric Analysis of a Heavy Water Electrolysis Experiment Using a Pd-B Alloy Cathode," *Proc. Electrochem. Soc.*, 2001-23, 194.
27. Srinivasan, M. *et al*. 1992. "Tritium and Excess Heat Generation During Electrolysis of Aqueous Solutions of Alkali Salts with Nickel Cathode," *Frontiers of Cold Fusion: Proceedings of the Third International Conference on Cold Fusion*, H. Ikegami, ed., October 21-25, Universal Academy Press, 123-138.
28. Szpak, S., Mosier-Boss, P.A., Young, C., and Gordon, F.E. 2005. "Evidence of Nuclear Reactions in the Pd Lattice," *Naturwissenschaften*, 92, 394-397.
29. Szpak, S., Mosier-Boss, P.A., and Gordon, F.E. 2007. "Further Evidence of Nuclear Reactions in the Pd/D Lattice: Emission of Charged Particles," *Naturwissenschaften*, 94, 511-514.
30. Mosier-Boss, P.A., Szpak, S., Gordon, F.E., and Forsley, L.P.G. 2007. "Use of CR-39 in Pd/D Co-Deposition Experiments," *Eur. Phys. J. Appl. Phys.*, 40, 293-303.
31. Szpak, S., Mosier-Boss, P.A., Boss, R.D., and Smith, J.J. 1998. "On the Behavior of the Pd/D System: Evidence for Tritium Production," *Fusion Technology*, 33, 38-51.
32. Szpak, S. *et al*. 2005. "The Effect of an External Electric Field on Surface Morphology of Co-deposited Pd/D Films," *J. Electroanal. Chem.*, 580, 284-290.
33. Will, F.G., Cedzynska, K., and Linton, D.C. 1994. "Tritium Generation in Palladium Cathodes with High Deuterium Loading," *Transactions of Fusion Technology*, 26, December, 209-213; Will, F.G. *et al*. 1993. "Reproducible Tritium Generation in Electrochemical Cells Employing Palladium Cathodes with High Deuterium Loading," *J. Electroanal. Chem.*, 360, 161-176.
34. Iwamura, Y., Sakano, M., and Itoh, T. 2002. "Elemental Analysis of Pd Complexes: Effects of D_2 Gas Permeation," *Jpn. J. Appl. Phys. A*, 41, 4642; Iwamura, Y. *et al*. 2005. "Observation of Surface Distribution of Products By X-Ray Fluorescence Spectrometry During D_2 Gas Permeation Through Pd Complexes," in *Proc. of the 12th International Conference on Condensed Matter Nuclear Science*, Yokohama, Japan.
35. Arata, Y. and Zhang, Y.C. 1999. "Anomalous Production of Gaseous ^{4}He at the Inside of DS-Cathode During D_2-Electrolysis," *Proc. Jpn. Acad. Ser. B*, 75, 281; Arata, Y. and Zhang, Y.C. 1999. "Observation of Anomalous Heat Release and Helium-4 Production from Highly Deuterated Fine Particles," *Jpn. J. Appl. Phys. Part 2*, 38, L774; Arata, Y. and Zhang, Y.C. 2008. "The Establishment of Solid Nuclear Fusion Reactor," *J. High Temp. Soc.*, 34, 2, 85.
36. Fleischmann, M. and Pons, S. 1993. "Calorimetry of the Pd-D_2O System: From Simplicity via Complications to Simplicity," *Physics Letters A*, 176, 118-129; Fleischmann, M. and Pons, S. 1989. "Electrochemically Induced Nuclear Fusion of Deuterium," *J. Electroanal. Chem.*, 261, 301-308, erratum, 263, 187; Fleischmann, M. and Pons, S. 1992. "Some Comments on the Paper 'Analysis of Experiments on Calorimetry of LiOD/D_2O Electrochemical Cells,' R.H. Wilson *et al.*," *J. Electroanal. Chem.*, 332, 1, 33-53.
37. Swartz, M. and Verner, G. 2006. "Excess Heat from Low Electrical Conductivity Heavy Water Spiral-Wound Pd/D_2O/Pt and Pd/D_2O-$PdCl_2$/Pt Devices," *Condensed Matter Nuclear Science: Proceedings of ICCF10*, P.L. Hagelstein and S.R. Chubb, eds., World Scientific Publishing, 29-44.
38. Swartz, M.R. 2008. "Excess Power Gain and Tardive Thermal Power Generation Using High Impedance and Codepositional Phusor Type LANR Devices," *Proc. of the Fourteenth International Conference on Cold Fusion* (in preparation).
39. Swartz, M. 1998. "Improved Electrolytic Reactor Performance Using p-Notch System Operation and Gold Anodes," *Transactions of the American Nuclear Association*, Nashville, TN Meeting, 78, 84-85.
40. Swartz, M. 1997. "Consistency of the Biphasic Nature of Excess Enthalpy in Solid State Anomalous Phenomena with the Quasi-1-Dimensional Model of Isotope Loading into a Material," *Fusion Technology*, 31, 63-74.
41. Swartz, M. and Verner, G. 2006. "Can a Pd/D_2O/Pt Device be Made Portable to Demonstrate the Optimal Operating Point?" *Condensed Matter Nuclear Science: Proceedings of ICCF10*, P.L. Hagelstein and S.R. Chubb, eds., World Scientific Publishing, 45-54.
42. Swartz, M. and Verner, G. 2006. "Photoinduced Excess Heat from Laser-Irradiated Electrically-Polarized Palladium Cathodes in D_2O," *Condensed Matter Nuclear Science: Proceedings of ICCF10*, P.L. Hagelstein and S.R. Chubb, eds., World Scientific Publishing, 213-226.
43. McKubre, M., Tanzella, F., Hagelstein, P., Mullican, K., and Trevithick, M. 2006. "The Need for Triggering in Cold Fusion Reactions," *Condensed Matter Nuclear Science: Proceedings of ICCF10*, P.L. Hagelstein and S.R. Chubb, eds., World Scientific Publishing.
44. Swartz, M. 1997. "Codeposition of Palladium and Deuterium," *Fusion Technology*, 32, 126-130.
45. Swartz, M. 1998. "Patterns of Failure in Cold Fusion Experiments," *Proceedings of the 33rd Intersociety Engineering Conference on Energy Conversion*, IECEC-98-I229, Colorado Springs, CO, August 2-6.
46. Violante, V., Castagna, E., Sibilia, C., Paoloni, S., and Sarto, F. 2006. "Analysis of Mi-Hydride Thin Film After Surface Plasmons Generation by Laser Technique," *Condensed Matter Nuclear Science: Proceedings of ICCF10*, P.L. Hagelstein and S.R. Chubb, eds., World Scientific Publishing.
47. Miley, G.H. and Shrestha, P. 2006. "Review of Transmutation Reactions in Solids," *Condensed Matter Nuclear Science: Proceedings of ICCF10*, P.L. Hagelstein and S.R. Chubb, eds., World Scientific Publishing.
48. Swartz, M.R., Verner, G., and Weinberg, A. 2007. "Possible Non-Thermal Near-IR Emission Linked with Excess Power Gain in High Impedance and Codeposition Phusor-LANR Devices," *Proc. of the Fourteenth International Conference on Cold Fusion* (in preparation).
49. Rabinowitz, M. *et al*. 1993. "Opposition and Support for Cold Fusion," *Proc. Fourth International Conference on Cold Fusion*, Lahaina, Maui, Electric Power Research Institute.
50. Swartz, M. 1997. "Phusons in Nuclear Reactions in Solids," *Fusion Technology*, 31, 228-236.
51. Swartz, M. and Verner, G. 1999. "Bremsstrahlung in Hot and Cold Fusion," *Journal of New Energy*, 3, 4, 90-101.
52. Swartz, M. 1993. Science and Engineering of Hydrided Metals Series, Volume 2, "Calorimetric Complications: The Examination of the Phase-II Experiment and Other Select Calorimetric Issues," Ed. JET Technology Press; Swartz, M. 1993. "Some Lessons from Optical Examination of the PFC Phase-II Calormetric Curves," Vol. 2, *Proceedings: Fourth International Conference on Cold Fusion*, 19-1, *op. cit.*
53. Swartz, M. 1994. "A Method to Improve Algorithms Used to Detect Steady State Excess Enthalpy," *Transactions of Fusion Technology*, 26, 156-159.
54. Swartz, M. 1992. "Quasi-One-Dimensional Model of Electrochemical Loading of Isotopic Fuel into a Metal," *Fusion Technology*, 22, 2, 296-300.
55. Swartz, M. 1994. "Isotopic Fuel Loading Coupled to Reactions at an Electrode," *Fusion Technology*, 26, 4T, 74-77.
56. Swartz, M. 2000. "Control of Low Energy Nuclear Systems through Loading and Optimal Operating Points," ANS/ 2000 International Winter Meeting, November 12-17, Washington, D.C.
57. Swartz, M. 1999. "Generality of Optimal Operating Point Behavior in Low Energy Nuclear Systems," *Journal of New Energy*, 4, 2, 218-228.
58. Swartz, M. 1998. "Optimal Operating Point Characteristics of Nickel Light Water Experiments," *Proceedings of ICCF7*.
59. Weiland, T. *et al*. 2001. "*Ab Initio* Numerical Simulation of Left-Handed Metamaterials: Comparison of Calculations and Experiments," *Journal of Applied Physics*, 90, 10, 5419-5424.
60. Haus, H.A. and Melcher, J.R. 1989. *Electromagnetic Fields and Energy*, Prentice-Hall.
61. Adler, R.B., Chu, L.J., and Fano, R.M. 1960. *Electromagnetic Energy Transmission and Radiation*, John Wiley & Sons, Inc.
62. Venermo, J. and Sihvola, A. 2005. "Dielectric Polarizability of Circular Cylinder," *Journal of Electrostatics*, 63, 2, 101-117.
63. Giordano, S. 2005. "Multipole Expansions; Composite Materials; Dielectric Homogenisation," *Journal of Electrostatics*, 63, 1, 1-19.
64. Ohshima, H. 1996. "Electrostatic Interaction Between Two Parallel Cylinders," *Colloid & Polymer Science*, 274, 12.
65. Cherstvy, A.G. and Winkler, R.G. 2004. "Complexation of Semiflexible Chains with Oppositely Charged Cylinder," *Journal of Chemical Physics*, 120, 19, 9394-9400. In the case for biopolymers, they found that sufficiently flexible chains prefer to wrap around a cylinder in a helical manner, when their charge density is smaller than that of the cylinder. The optimal value of the helical pitch is found by minimization of the sum of electrostatic and bending energies.

66. Scharstein, R.W. 2007. "Capacitance of a Tube," *Journal of Electrostatics*, 65, 1, 21-29.
67. Dumitran, L.M. *et al*. 2006. "2-D Corona Field Computation in Configurations with Ionising and Non-Ionising Electrodes," *Journal of Electrostatics*, 64, 3-4, 176-1 86.
68. Smith, J.R. 1999. "Electric Field Imaging," Thesis, Doctor of Philosophy, Massachusetts Institute of Technology.
69. Chien, C.B. and Pine, J. 1991. "Voltage-sensitive Dye Recording of Action Potentials and Synaptic Potentials from Sympathetic Microcultures," *Biophys. J.*, 3, 60, 697-711.
70. Cowgill, D.F. 1980. "Dynamic Ion Beam Method for Measuring Deuterium Diffusion in Films," *IEEE Transactions on Nuclear Science*, NS-28, 2, 1851-1185.
71. Bandourko, V. 1996. "Deuterium Permeation Through Nb During Low Energy Ion Irradiation at Controlled Surface Conditions," *Journal of Nuclear Materials*, 233-237 (PART II), 1184-1188.
72. Tanabe, T., Hachino, H., and Takeo, M. 1990. "Behavior of Deuterium Implanted in Mo," *Journal of Nuclear Materials*, 176-77, 666-671.
73. Bockris, J. O'M. and Reddy, A.K.N. 1970. *Modern Electrochemistry*, Plenum Press.
74. Uhlig, H.H. 1971. *Corrosion and Corrosion Control*, Wiley.
75. Szpak, S., Gabriel, C.J., Smith, J.J., and Nowak, R.J. 1991. "Electrochemical Charging of Pd Rods," *J. Electroanal. Chem.*, 309, 273-292.
76. Viitanen, M. 1993. "A Mathematical Model of Metal Hydride Electrodes," *J. Electrochem. Soc.*, 140, 4, 936-942.
77. Melcher, J.R. 1981. *Continuum Electromechanics*, MIT Press.
78. Von Hippel, A., Knoll, D.B., and Westphal, W.B. 1971. "Transfer of Protons through 'Pure' Ice 1h Single Crystals," *J. Chem. Phys.*, 54, 134, (also 145).
79. Swartz. M. 2002. "Dances with Protons: Ferroelectric Inscriptions in Water/Ice Relevant to Cold Fusion and Some Energy Systems," *Infinite Energy*, 8, 44, 64-70.
80. Hampel, C.A. 1954. *Rare Metal Handbook*, Reinhold Publishing.
81. Hansen, M. and Anderko, K. 1958. *Constitution of Binary Alloys*, McGraw-Hill.
82. Vogt, H. and Balzer, R.J. 2005. "The Bubble Coverage of Gas-evolving Electrodes in Stagnant Electrolytes," *Electrochimica Acta*, 50, 10, 2073-2079.
83. Wuthrich, R., Comninellis, C., and Bleuler, H. 2005. "Bubble Evolution on Vertical Electrodes Under Extreme Current Densities," *Electrochimica Acta*, 50, 25/26, 5242-5246.
84. Wuthrich, R., Fascio, V., and Bleuler, H. 2004. "A Stochastic Model for Electrode Effects," *Electrochimica Acta*, 49, 22/23, 4005-4010.
85. Iwasaki, A., Kaneko, H., Abe, Y., and Kamimoto, M. 1998. "Investigation of Electrochemical Hydrogen Evolution Under Microgravity Condition," *Electrochimica Acta*, 43, 5/6, 509-514.
86. Matsushima, H. *et al*. 2003. "Water Electrolysis Under Microgravity: Part 1. Experimental Technique," *Electrochimica Acta*, 48, 28, 4119-4125.
87. Mat, M.D., Aldas, K., and Ilegbusi, O.J. 2004. "A Two-phase Flow Model for Hydrogen Evolution in an Electrochemical Cell," *International Journal of Hydrogen Energy*, 29, 10, 1015-1023.
88. Gabrielli, C., Huet, F., and Nogueira, R.P. 2002. "Electrochemical Impedance of H_2-evolving Pt Electrode Under Bubble-induced and Forced Convections in Alkaline Solutions," *Electrochimica Acta*, 47, 13/14, 2043-2048.
89. Correia, A.N. and Machado, S.A.S. 1998. "Hydrogen Evolution on Electrodeposited Ni and Hg Ultramicroelectrodes," *Electrochimica Acta*, 43, 3/4, 367-373.
90. Mosier-Boss, P.A., Szpak, S., Gordon, F.E., and Forsley, L.P.G. 2008. "Triple Tracks in CR-39 as the Result of Pd-D Co-deposition: Evidence of Energetic Neutrons," *Naturwissenschaften*, doi:10.1007/s00114-008-0449-x.

About the Author
Mitchell R. Swartz has the degrees of BSEE, MSEE, EE, and ScD in Electrical Engineering from the Massachusetts Institute of Technology and an MD from Harvard Medical School. He served surgical internship and radiation oncology residency at the Massachusetts General Hospital. From the Laboratory for Insulation Research at MIT through biomedical engineering work at MIT and the Boston hospitals, including development of PET scans for imaging of human tumors, he continues research on dielectrics, lattice assisted nuclear studies, and the interaction of radiation with materials for the production of electronic and hydrogen flux devices for use in propulsion, electricity production systems, and artificial internal organs.

*Email: mica@theworld.com